Electronic Supplementary Material (ESI) for Journal of Materials Chemistry C.
This journal is © The Royal Society of Chemistry 2022

Supplementary Information

Nanocomposites of chalcogenide phase-change materials: from C-doping of thin films to advanced multilayers

Rebecca Chahine,[a] Martina Tomelleri,[a] Jessy Paterson,[a] Mathieu Bernard,[a] Nicolas Bernier,[a] François Pierre,[a] Denis Rouchon,[a] Audrey Jannaud,[a] Cristian Mocuta,[b] Valentina M. Giordano,[c] Françoise Hippert,[d] and Pierre Noé[a,*]

[a] Université Grenoble Alpes, CEA, LETI, Grenoble F-38000, France.
[b] Synchrotron SOLEIL, F-91192 Gif-sur-Yvette, France.
[c] ILM, UMR 5306 Univ. Lyon 1-CNRS, Villeurbanne Cedex F-69622, France.
[d] Université Grenoble Alpes, CNRS, Grenoble INP, LMGP, Grenoble F-38000, France.
* Email: : pierre.noe@cea.fr

1/Time of flight secondary ion mass spectrometry (ToF-SIMS) depth profiles of as-deposited GeTe/C and $Ge_2Sb_2Te_5$/C multilayer films.

Amorphous as-deposited GeTe/C and $Ge_2Sb_2Te_5$(GST)/C multilayers (MLs) with nominal GeTe or GST layer thickness of 4 nm and C layer thickness of 0.5, 1 or 2 nm were characterized by ToF-SIMS. The measurements were performed on a Tof-SIMS 5 (IONTOF GmbH) dual beam instrument equipped with a bismuth liquid metal ion gun (LMIG) used for analysis and a cesium sputter source for sample erosion. A 15 keV Bi^+ pulsed beam at 15 keV was rastered over an analysis area of 60 x 60 µm2 centered in the middle of the sputter crater of 200 × 200 µm^2 generated by a 500 eV Cs^+ beam. Both beams were incident at approximately 45°. The insulating nature of the silicon oxide substrate induces sample charging during measurements. A low-energy electron flood gun was used for charge compensation. The negative ion depth profiles were acquired in non-interlaced mode by alternating data acquisition, sputtering and charge compensation cycles. All the data were recorded and analyzed by the SurfaceLab 6 software from IONTOF GmbH.

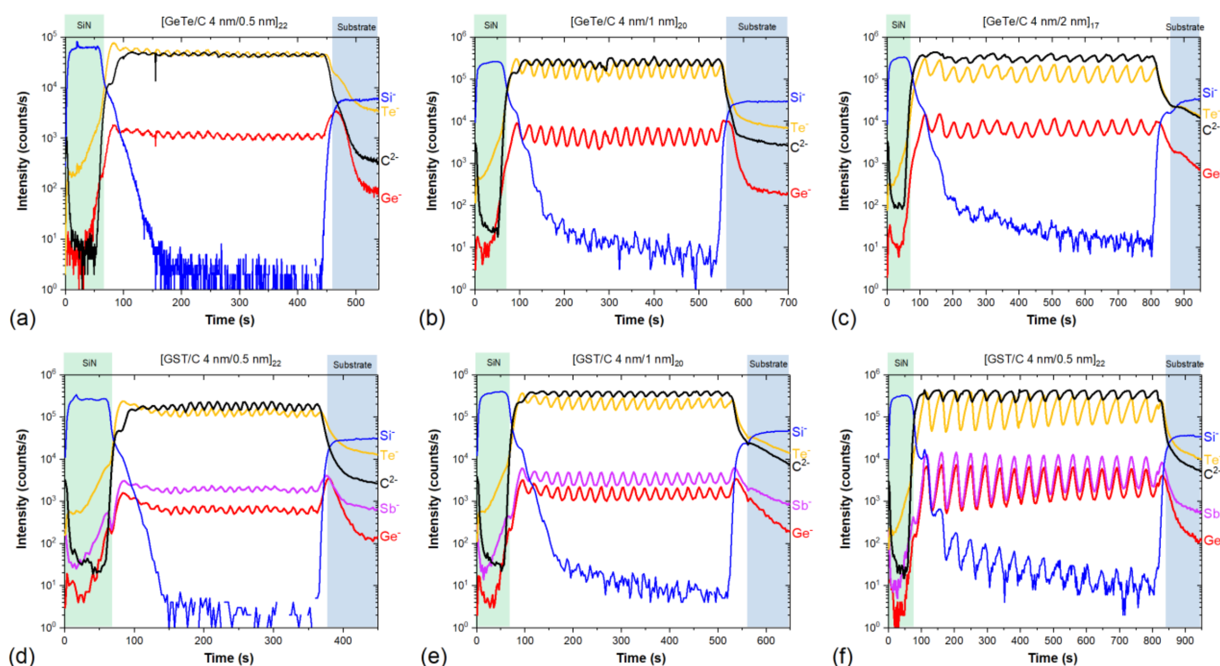

Figure S1. ToF-SIMS depth profiles as a function of the sputtering time for as-deposited (**a**) [GeTe 4nm /C 0.5nm]$_{22}$, (**b**) [GeTe 4nm /C 1nm]$_{20}$, (**c**) [GeTe 4nm /C 2nm]$_{17}$, (**d**) [$Ge_2Sb_2Te_5$ 4nm /C 0.5nm]$_{22}$, (**e**) [$Ge_2Sb_2Te_5$ 4nm /C 1nm]$_{20}$ and (**f**) [$Ge_2Sb_2Te_5$ 4nm /C 2nm]$_{17}$ multilayers deposited on a Si substrate covered by a 500 nm thick SiO2 layer (obtained by thermal oxidation of the Si substrate) and capped by a 10 nm thick SiN layer. The Si^- profile allows to determine the limits of the GeTe/C or $Ge_2Sb_2Te_5$/C stack. For all multilayers, the number of periods coincides with the nominal one. The signal of species close to the interfaces with the SiO_2 substrate and SiN capping layer is altered due to roughness and/or change of abrasion yield. Oscillations of the Ge-,Te- and Sb- profiles are perfectly in phase and clearly shifted with respect to the oscillations of the C- profile. However, note that the oscillations of C- are not perfectly shifted of 180°C with respect to those of PCM layer species. This artefact is due to a significant change in abrasion yield, resulting from huge difference in material density between PCM and C layers, coupled with interface roughness.

Supplementary Information

2/Composition of C-doped GeTe and $Ge_2Sb_2Te_5$ films and GeTe/C and $Ge_2Sb_2Te_5$/C multilayer films

The number of Ge, Sb, Te and Ar per cm^2 was measured by ion beam analysis techniques using Rutherford backscattering spectrometry (RBS) combined with particle-induced x-ray emission (PIXE) in order to determine separately the number of Sb and Te atoms. RBS only allows to measure the total number of Sb and Te atoms. The number of C per cm^2 was determined by nuclear reaction analysis (NRA). The NRA intensity was calibrated by comparison with a reference C-implanted Si sample. The contribution of the C contamination caused by the analysis was subtracted. All measurements were performed at Arcane (CENBG, Gradignan, France). The analysed surface is of the order of a few mm^2. Results are given in **Table S2**. The presence of a small amount of Ar in all films results from the sputtering deposition method.

The ratio between the numbers of Ge and Te atoms is the same within the error bars in all C-doped GeTe films and GeTe/C MLs. Its average value is 1.18 ± 0.1. There is an excess of Ge, as usually the case for films deposited by sputtering from a GeTe target.

The ratios between the numbers of the Ge, Te and Sb atoms are the same within the error bars in all C-doped GST films and GST/C MLs. The composition of the deposited Ge-Sb-Te phase is close to the target composition, $Ge_2Sb_2Te_5$, although a small Te deficiency is present. The average ratio between the numbers of Ge and Sb atoms is 1.04 ± 0.1. The average ratio between the numbers of Sb and Te atoms is 0.43 ± 0.04 and the ratio between the numbers of Ge and Te atoms is 0.45 ± 0.04, to be compared to expected values of 0.4.

Sample label	Ge	ΔGe	Sb	ΔSb	Te	ΔTe	C	ΔC
GeTe doped with 6.5 at.% C	166	±7.6			140.5	±6.0	21.5	±1.3
GeTe doped with 10.4 at.% C	172.2	±7.9			145.5	±6.3	36.9	±2.2
GeTe doped with 18.8 at.% C	160	±7.4			136.3	±5.9	68.6	±4.1
GeTe doped with 25.1 at.% C	158	±7.3			131.4	±5.6	96.9	±5.8
[GeTe 4 nm/ C 0.5 nm]$_{22}$	155.3	±7.1			133	±5.7	75.2	±4.5
[GeTe 4 nm/C 1 nm]$_{20}$	147	±6.8			124.4	±5.3	146.6	±8.8
[GeTe 4 nm/C 2 nm]$_{17}$	124	±5.7			107.5	±4.6	257	±15.4
GST doped with 5.8 at.% C	69.5	±3.2	69.0	±3.0	155.7	±6.7	18.2	±1.1
GST doped with 11.5 at.% C	70.5	±3.2	67.5	±2.9	157.5	±6.8	38.6	±2.3
GST doped with 17.9 at.% C	61	±2.8	60.0	±2.6	134.7	±5.8	55.7	±3.3
GST doped with 24.5 at.% C	58.2	±2.7	53.9	±2.3	130.9	±5.6	78.9	±4.7
[GST 4 nm/C 0.5 nm]$_{22}$	64.9	±3.0	60.8	±2.6	142.3	±6.1	70.9	±4.3
[GST 4 nm/C 1 nm]$_{20}$	57.4	±2.6	54.8	±2.4	126.8	±5.5	152.6	±9.2
[GST 4 nm/C 2 nm]$_{17}$	52.5	±2.4	51.8	±2.2	115.7	±5.0	253.1	±15.2

Table S2. Number of atoms (in 10^{15} at/cm^2) in C-doped GeTe and $Ge_2Sb_2Te_5$ (GST) films and in GeTe/C and $Ge_2Sb_2Te_5$(GST)/C multilayers.

3/FTIR spectra of amorphous and crystallized GeTe films

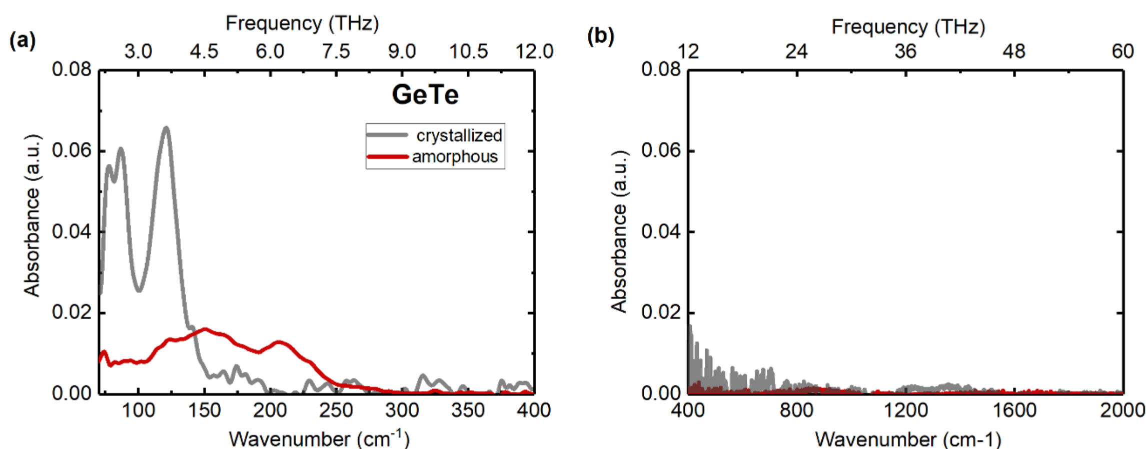

Figure S3. Room temperature FTIR absorbance spectra in the 70-400 cm-1 range (**a**) and in the 400-2000 cm-1 range (**b**) of a 150 nm thick GeTe film in the amorphous as-deposited state (red lines) and in the crystalline state (grey lines). The film was deposited at room temperature on a Si substrate. A piece of the film was then crystallized by heating up to 400°C at a rate of 10°C/min and cooling down to room temperature in a few minutes. The absorbance spectrum of the Si substrate has been subtracted. No vibration modes are detected above 250 cm^{-1} neither in the amorphous nor in the crystalline GeTe phase.

4/Sheet resistance of GeTe/C and $Ge_2Sb_2Te_5$/C multilayers.

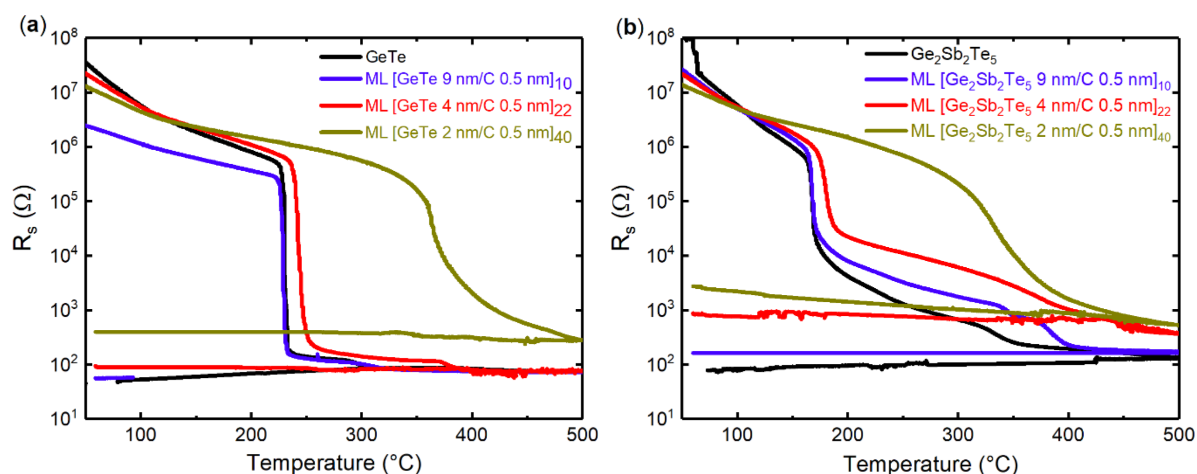

Figure S4. Sheet resistance as a function of temperature when heating up to 500°C and cooling (ramp rate of 10°C/min) for (**a**) GeTe/C and (**b**) $Ge_2Sb_2Te_5$ (GST)/C multilayer (ML) films with a C layer thickness equal to 0.5 nm. The as-deposited multilayers are amorphous. The crystallization temperature Tx of multilayers with 9 nm thick GeTe or GST layers is equal to that of the reference 100 nm thick GeTe or GST films. A moderate increase in Tx of about 13°C occurs when the thickness of the phase change material layer decreases to 4 nm. By contrast, a large increase (by 120°C for GeTe and 150°C for GST) occurs when the thickness of the GeTe or GST layer in the multilayer decreases from 4 to 2 nm.

Supplementary Information

5/Crystallization of excess Ge in GeTe/C multilayers

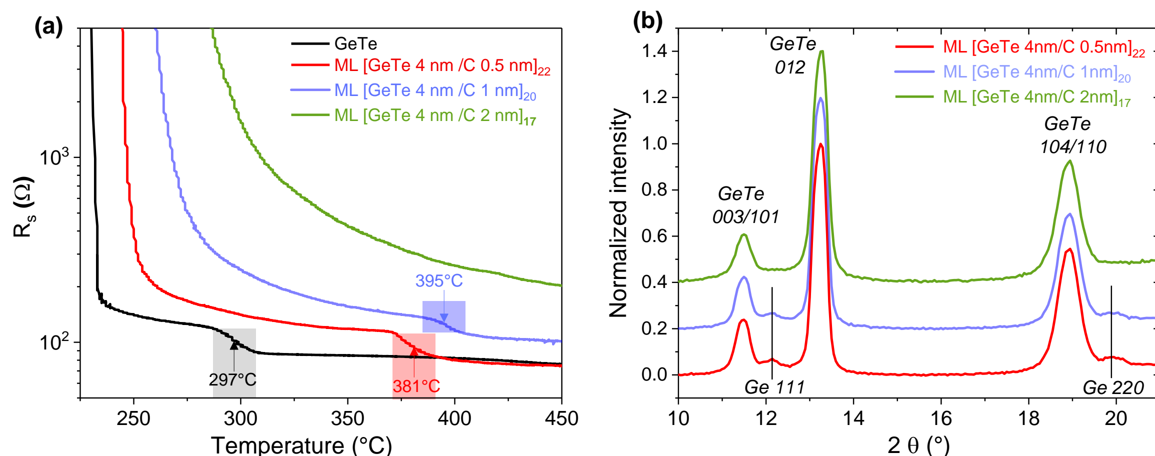

Figure S5. (**a**) Enlarged view of the sheet resistance curves of **Fig. 3(a)** in the temperature range where the excess Ge crystallizes. The heating rate was 10°C/min. The crystallization of Ge leads to a small drop of resistivity in a 20°C range around 297°C in the reference GeTe film, around 381°C in the [GeTe 4 nm/C 0.5 nm]$_{22}$ multilayer and around 395°C in the [GeTe 4 nm/C 1 nm]$_{20}$ multilayer. No resistivity drop is detected in the [GeTe/C 4 nm/2 nm]$_{17}$ multilayer. (**b**) In-plane X-ray diffraction patterns (λ =0.6908 Å) at room temperature for GeTe/C multilayers previously annealed by heating at 425°C at a rate of 10°C/min followed by rapid cooling in a few minutes. *111* and *220* Ge diffraction peaks are detected in the [GeTe 4 nm/C 0.5 nm]$_{22}$ and in the [GeTe 4 nm/C 1 nm]$_{20}$ multilayers but not in the [GeTe 4 nm/C 2 nm]$_{17}$ multilayer.

6/Scanning transmission electron microscopy (STEM) images of GeTe/C multilayer films

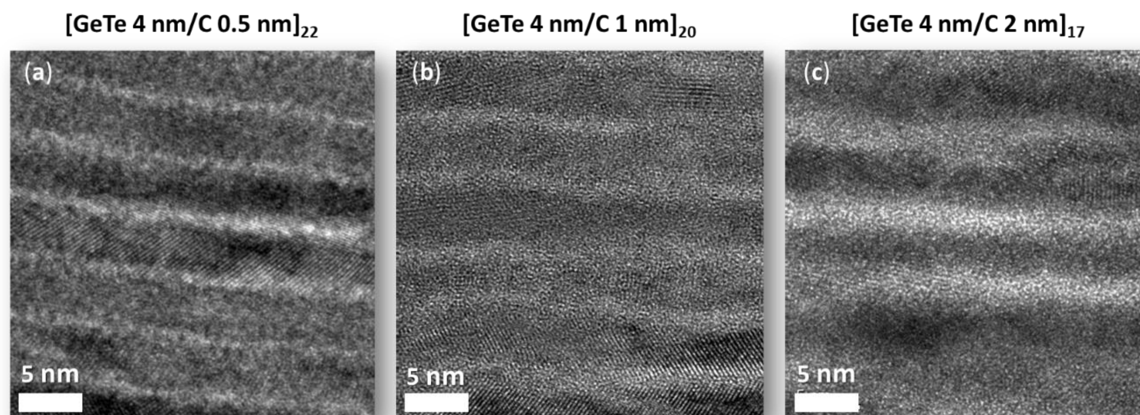

Figure S6. Cross section BF-STEM images of the [GeTe 4 nm /C 0.5 nm]$_{22}$ ML (**a**), [GeTe 4 nm /C 1 nm]$_{20}$ ML (**b**) and the [GeTe/C 4 nm/2 nm]$_{17}$ ML (**c**). After deposition, the ML films were heated up to 300°C in a few minutes, held at 300° for 15 minutes and then cooled down to room temperature in a few minutes. Bright C layers alternate with darker GeTe layers.

Supplementary Information

7/X-ray Diffraction (XRD)

7.1/ Comparison of out-of-plane and in-plane XRD patterns measured at room temperature in GeTe/C multilayers, in a GeTe film and in a C-doped GeTe film.

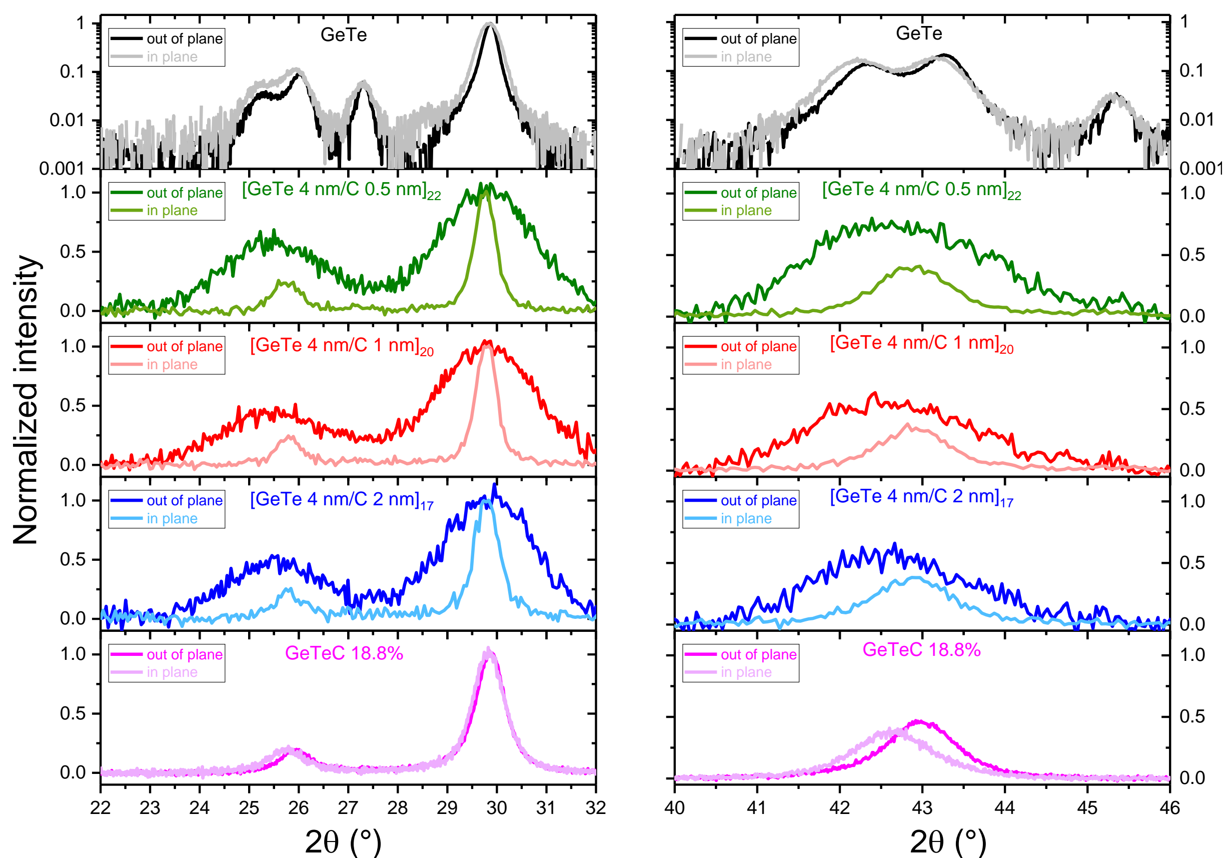

Figure S7. Comparison of out-of-plane and in-plane x-ray diffraction patterns (λ =1.542 Å, Cu Kα radiation) at room temperature in selected 2θ ranges for a GeTe film, GeTe/C MLs and a C-doped GeTe film (C content 18.8±1.1 at %). All films were previously annealed at 425°C. In-plane diffraction probes lattice planes that are nearly perpendicular to the film surface, while out-of-plane diffraction probes lattice planes that are parallel to the film surface The intensities have been normalized to facilitate the comparison. For $2\theta \approx 30°$, the instrumental contribution to the full width at half maximum of the peak is 0.18° for the MLs and 0.1° for the GeTe and C-doped GeTe films in the out-of-plane geometry and 0.3° for all samples in the in-plane geometry.

In the GeTe films, the XRD patterns measured in the two diffraction conditions are similar (same position and same width of the diffraction peaks and same intensity ratios). The observation of similar intensity ratios reveals negligible texture effects and thus a random distribution of crystallite orientations in the film.

In the crystallized ML films, the position of the 012 diffraction peak ($2\theta \approx 30°$) is almost the same in the two diffraction conditions but there are systematic shifts in the positions of the maxima of the broad peaks corresponding to the 003/101 doublet (in the 2θ range [23-27.5°]) and to the 104/110 doublet (in the 2θ range [40-45°]). This can be explained by texture effects leading to changes of the relative intensity of the two peaks of each doublet. For out-of-plane diffraction, the 003 peak is more intense than the 101 peak and the 104 peak more intense than the 110 peak. For in-plane diffraction, the trend is opposite. Thus, the comparison of out-of-plane and in-plane x-ray diffraction patterns of GeTe/C multilayers allows to demonstrate that the GeTe phase is rhombohedral at room temperature in 4 nm thick GeTe layers.

The same conclusion applies to all the crystallized C-doped GeTe films studied, as shown in **Fig. S7** for the film containing 18.8 at.% C. (In C-doped GeTe films, the 003 peak is less intense than the 101 peak and the 104 peak less intense than the 110 peak for out-of-plane diffraction and the trend is opposite for in-plane diffraction). In the literature, the structure of the GeTe phase in crystallized C-doped GeTe films has been reported to be cubic (X. Biquard et al, Effect of doping on global and local order in crystalline GeTe, Applied Physics Letters, 2011, **98**, 231907). The present results show unambiguously that this conclusion was erroneous. However, a quantitative determination of the rhombohedral distortion is made impossible by the large width of the diffraction peaks.

Supplementary Information

7.2/XRD as a function of temperature for the [GeTe 4 nm/C 0.5 nm]$_{22}$ multilayer film

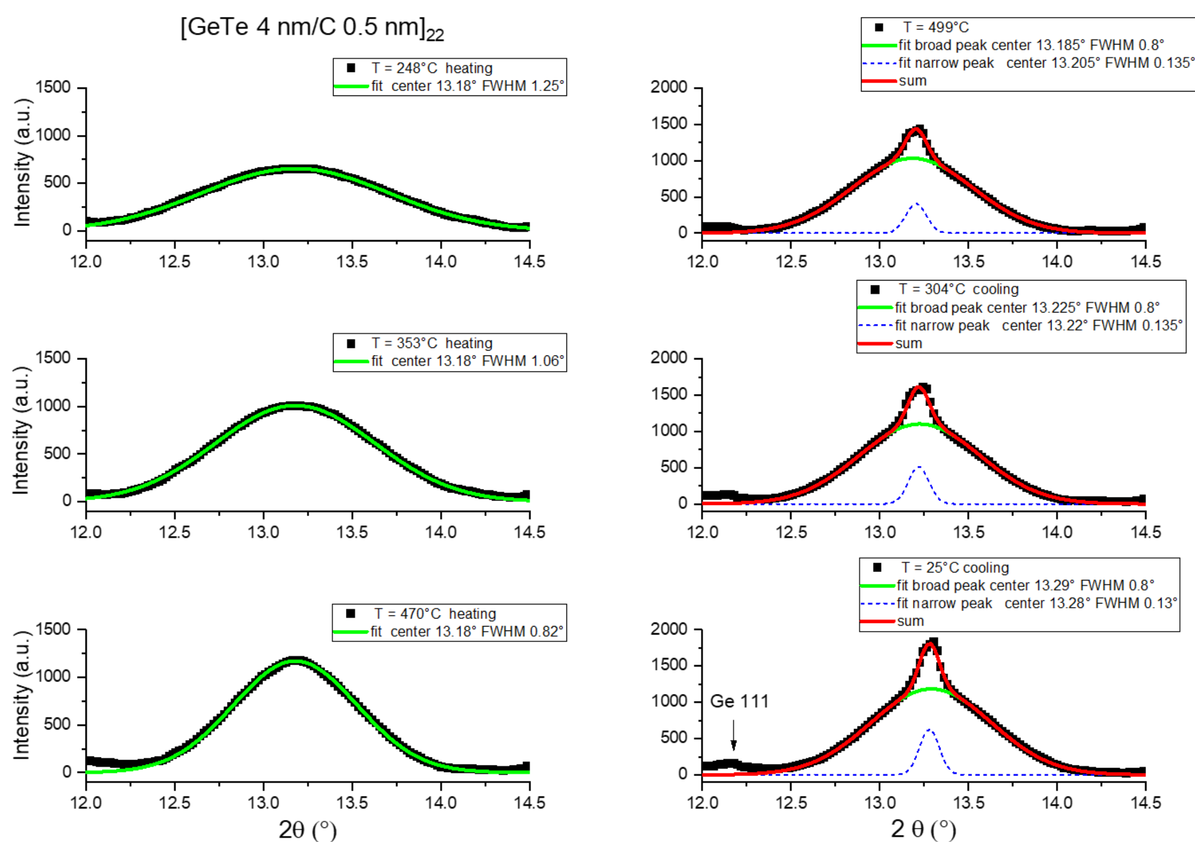

Figure S8. X-ray diffraction patterns (λ =0.6908 Å) for the [GeTe 4 nm/C 0.5 nm]$_{22}$ multilayer film in the 2θ range corresponding to the 012 peak of the rhombohedral α-GeTe phase (200 peak of the cubic β-GeTe phase) at selected temperatures. Gaussian fits are shown as solid lines. The initially amorphous ML film was heated up to 500°C at a rate of 2°C/min and cooled down at a rate of 20°C/min. Upon heating, a broad diffraction peak appears at 230°C. Its width decreases when the temperature increases. A narrow diffraction peak appears at 476°C upon heating. It is superimposed on the broad peak that was already present for lower temperatures. This narrow peak is detected in all diffraction patterns measured during heating from 476°C to 500°C and during cooling. At a given temperature, the centers of the narrow and broad peaks coincide. During cooling, the ratio of the areas of the narrow and broad peaks remains constant $\approx 8 \pm 1$ %. The presence of a narrow peak reveals that the 0.5 nm thick C layers have been locally destroyed by heating above 476°C and that some GeTe crystallites have grown coherently through several periods of the initial multilayer structure.

Supplementary Information

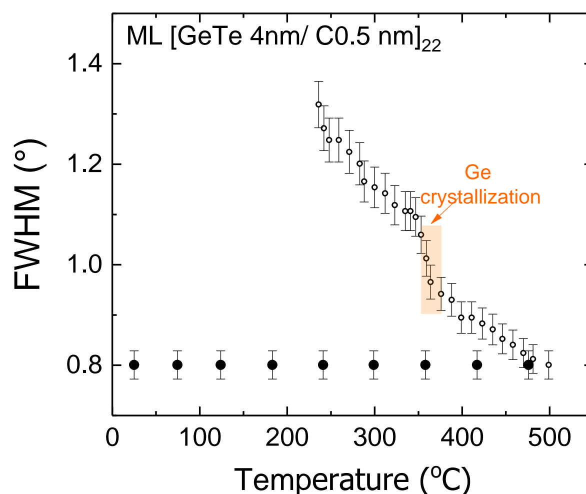

Figure S9. Measured Full Width at Half Maximum (Γ_{meas}) of the broad 012 peak of the rhombohedral α-GeTe phase (200 peak of the cubic β-GeTe phase) for x-ray diffraction patterns measured at λ =0.6908 Å as a function of temperature. The initially amorphous [GeTe 4 nm/C 0.5 nm]$_{22}$ multilayer film was heated up to 500°C at a rate of 2°C/min and cooled down at a rate of 20°C/min. The diffracting coherent domain (DCD) shown in **Fig. 5(a)** was estimated by a Scherrer analysis. The DCD value was calculated as $\frac{0.9*\lambda}{\Gamma*cos(\theta)}$ with Γ the full width at half maximum (FWHM) of the peak, after removing the contribution of the instrument from the measured full width at half maximum (Γ_{meas}). A possible contribution of inhomogeneous strains to the width of the peak can be neglected considering the small DCD values. The peak profile is Gaussian. Thus, $\Gamma = \sqrt{\Gamma_{meas}^2 - \Gamma_{instr}^2}$ with Γ_{instr} the instrument contribution equal to 0.05°. Its contribution is negligible

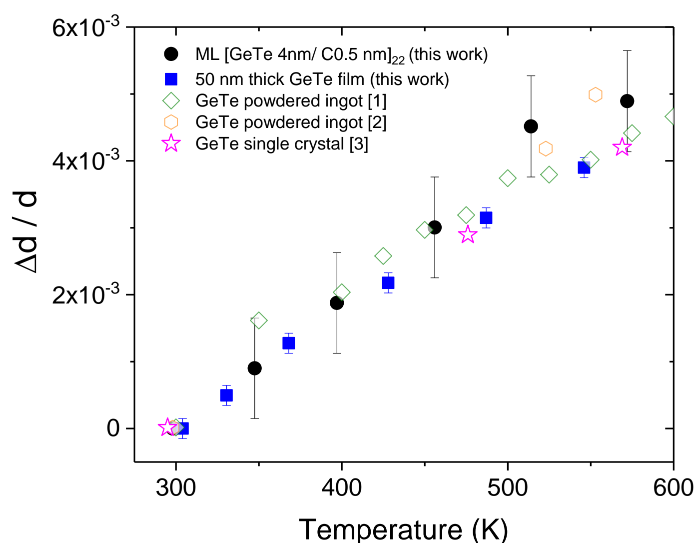

Figure S10. Relative change of the interplanar spacing of (012) planes as a function of temperature for the [GeTe 4 nm/C 0.5 nm]$_{22}$ multilayer and the reference 50 nm thick GeTe film (present work) compared to literature results. $\Delta d/d$ was calculated from the lattice parameters given in Refs [1,2,3]. The comparison is restricted to the temperature range where the GeTe phase is rhombohedral. The transition to the cubic β-GeTe phase occurs at 640 K for the ingot of Ref [1], 648 K for the ingot of Ref [2], 705 K for the single crystal of Ref.[3] and about 700 K for the GeTe film (this work).

[1] E. M. Levin, M. F. Besser and R. Hanus, Electronic and thermal transport in GeTe: A versatile base for thermoelectric materials, *J. of Appl. Physics*, 2013, **114**, 083713.
[2] H. Wiedemeier and P. A. Siemers, The Thermal Expansion of GeS and GeTe, *Z. Anorg. Allg. Chem.*, 1977, **431**, 299-304.
[3] T. Chattopadhyay, J.-X. Boucherle and H. G. von Schnering, Neutron diffraction study on the structural phase transition in GeTe, *J. Phys. C: Solid State Phys.*, 1987, **20**, 1431-1440.

Supplementary Information

7.3/ Determination of the average crystallite size in GeTe/C and GST/C multilayers and in C-doped GeTe and GST films

Out-of-plane and in-plane x-ray diffraction patterns were systematically measured (λ =1.542 Å, Cu Kα radiation) at room temperature in all GeTe/C and GST/C MLs and C-doped GeTe and GST films previously annealed at 425°C, as shown in **Fig. S7** for selected films. The diffracting coherent domain (DCD) was estimated by a Scherrer analysis of the width of the 012 diffraction peak for GeTe and the 200 diffraction peak for GST. The results are shown in **Fig.7**. For in-plane diffraction, the DCD value is related to the average grain size in the plane of the film, while for out-of-plane diffraction it is related to the average grain size along the normal to the film.

The DCD value was calculated as $\frac{0.9*\lambda}{\Gamma*cos(\theta)}$ with Γ the full width at half maximum (FWHM) of the peak, after removing the contribution of the instrument from the measured full width at half maximum (Γ_{meas}). A possible contribution of inhomogeneous strains to the width of the peak can be safely neglected in the case of out-of plane geometry in view of the small DCD values. It was not taken into account when calculating the in-plane DCD values.

For multilayers in the out-of-plane geometry, the peak profile is Gaussian and $\Gamma = \sqrt{\Gamma_{meas}^2 - \Gamma_{inst}^2}$ (with Γ_{inst}= 0.18°). For multilayers in the in-plane geometry, the peak profile is close to a Lorentz function and $\Gamma = \Gamma_{meas} - \Gamma_{inst}$ (with $\Gamma_{\mathrm{inst}} = 0.3°$). For C doped films, the peak profile is close to a Lorentz function in both in-plane and out-of-plane and geometries and $\Gamma = \Gamma_{meas} - \Gamma_{inst}$ (with $\Gamma_{\mathrm{inst}} = 0.3°$ for all films in the in-plane geometry and $\Gamma_{\mathrm{inst}} = 0.1°$ for C-doped films and $\Gamma_{\mathrm{inst}} = 0.18°$ for C-doped GST films in the out-of-plane geometry).

8/Room temperature Raman spectra of GeTe/C MLs

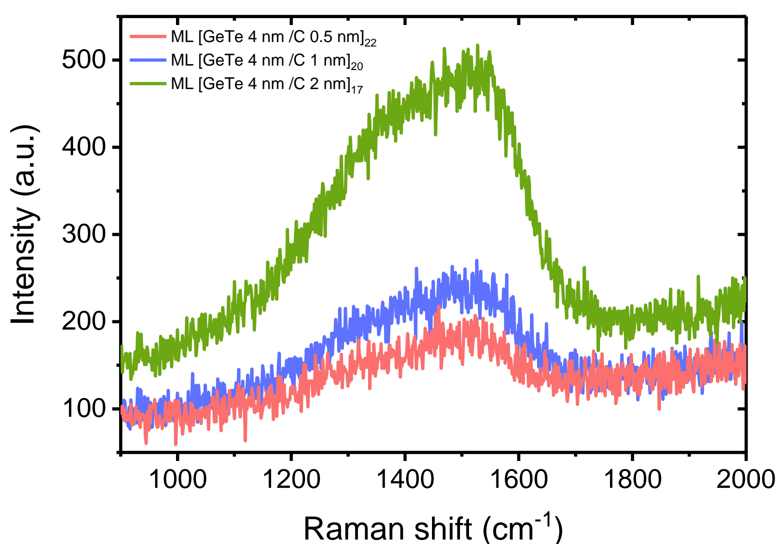

Figure S11. Room temperature Raman scattering spectra of GeTe/C multilayers annealed at 425°C showing the presence of an amorphous carbon phase (for experimental details see main text).